High-resolution measurement of the pressure broadening and shift of the Cs $D1$ and $D2$ lines by N_2 and He buffer gases

A. Andalkar* and R. B. Warrington†
Department of Physics, Box 351560, University of Washington, Seattle, Washington 98195-1560
(Received 14 September 2001; published 13 February 2002)

We have measured the pressure broadening and shift of the cesium $D1$ (894 nm) and $D2$ (852 nm) lines by nitrogen and helium buffer gases at pressures of 0–160 Torr using high-resolution spectroscopy with tunable external-cavity diode lasers. This measurement has a precision of about 1%, which significantly improves upon previously published measurements for the Cs $D1$ and $D2$ lines in N_2 and He buffer gases.

DOI: 10.1103/PhysRevA.65.032708 PACS number(s): 34.20.−b, 32.70.Jz

I. INTRODUCTION

The broadening and shift of atomic spectral lines by collisions with neutral atoms has been studied extensively since the very beginning of atomic physics [1–3], especially in systems such as the alkali metals and noble gases, which are important in the field of optical pumping. However, for the particular case of cesium, there are relatively few published studies of pressure broadening. Most of these measurements date from the era of Fabry-Perot and diffraction grating spectrometers, and the enormous advances in tunable laser technology over the past two decades have previously seen little application for this element. We have measured the pressure broadening and shift of the cesium $D1$ (894 nm) and $D2$ (852 nm) lines by nitrogen and helium buffer gases at pressures of 0–160 Torr using high-resolution laser spectroscopy with tunable external-cavity diode lasers. These measurements have a precision of about 1%, a significant improvement over previously published values, and include a significant correction to the only published values for the broadening of the $D1$ and $D2$ lines in nitrogen. This improvement is due primarily to the use of narrow-linewidth diode lasers, eliminating a major source of systematic uncertainty in previous measurements.

The most recent comprehensive measurements of the broadening and shift of the cesium $D1$ and $D2$ lines by N_2, H_2, and the noble gases at pressures up to 150 Torr are by Bernabeu and Alvarez [4]. This work, along with several more recent (but less comprehensive) measurements of the broadening and shift of cesium lines [5–7], used Fabry-Perot spectrometers with stated instrumental functions as wide as 1500 MHz. This is greater than the excited state hyperfine splitting in both the $D1$ and $D2$ lines ($\Delta\nu_{\rm hfs}=1168$ MHz in the $6P_{1/2}$, $\Delta\nu_{\rm hfs}=151$, 201, 251 MHz in the $6P_{3/2}$), and in fact is equal to the measured linewidths at buffer gas pressures of only 40–60 Torr. Deconvolution of this large instrumental function is the major source of systematic uncertainty in these measurements. We are aware of only one other cesium study using laser spectroscopy [8], made on the $D2$ line for the noble gases only.

The motivation for the present measurement comes from our work on spontaneous spin polarization in cesium [9,10]. Early on in that experiment, we realized that our observed linewidths in a number of sealed vapor cells with N_2 pressures of 20–75 Torr were 30–40 % narrower than the values expected based on the coefficients in Ref. [4]. Therefore, we decided to do a brief pressure broadening measurement using the 894 and 852 nm diode lasers already set up for the spontaneous polarization experiment.

II. EXPERIMENTAL APPARATUS

A gas-feed cesium vapor cell was built to allow the recording of resonance line transmission spectra over a range of pressures and for several different buffer gases. The cell itself was a 3 cm diameter, 3 cm long Pyrex cylinder, with a tubulation extending from one side for connection to the vacuum system. A rotatable joint with a clamped O-ring seal allowed rotation of the cell out of the beam path to facilitate background subtraction (see Sec. III). The cell was attached to a small glass vacuum system, evacuated by a turbomolecular pump backed by a mechanical rotary pump. A liquid nitrogen cold trap prevented any backstreaming of pump oils or other contaminants into the vacuum system and also prevented contamination of the pumping system by cesium vapor.

Typical system pressure with the cesium cell and gas-feed line both closed off was about 3×10^{-7} Torr. The cell remained at room temperature (about 21 °C) throughout the measurements, producing an equilibrium cesium vapor pressure of about 9×10^{-7} Torr and a number density of 3×10^{10} cm^{-3}. The temperature was monitored with a resolution of 0.1 °C using a type-K thermocouple probe affixed beside the cell, with a mercury lab thermometer providing a second independent measurement.

The gases came from standard high-pressure cylinders of high-purity N_2 or He, regulated down to about 10 psi (gauge) and then fed to a second regulator, this one with a 0–760 Torr absolute pressure gauge. An oxygen/moisture trap (Matheson 6427-4S) with a rated efficiency of 20 parts per billion (ppb) prevented O_2 or H_2O contaminants in the gas from consuming the cesium vapor in the cell. Pressure measurement of the buffer gas with a large mercury manometer provided resolution of about 0.5 Torr. The mercury manometer has one major advantage over other pressure sensors, in that any possible systematic error in pressure measurement is

*Electronic address: andalkar@u.washington.edu
†Present address: CSIRO Telecommunications and Industrial Physics, Lindfield NSW 2070, Australia.

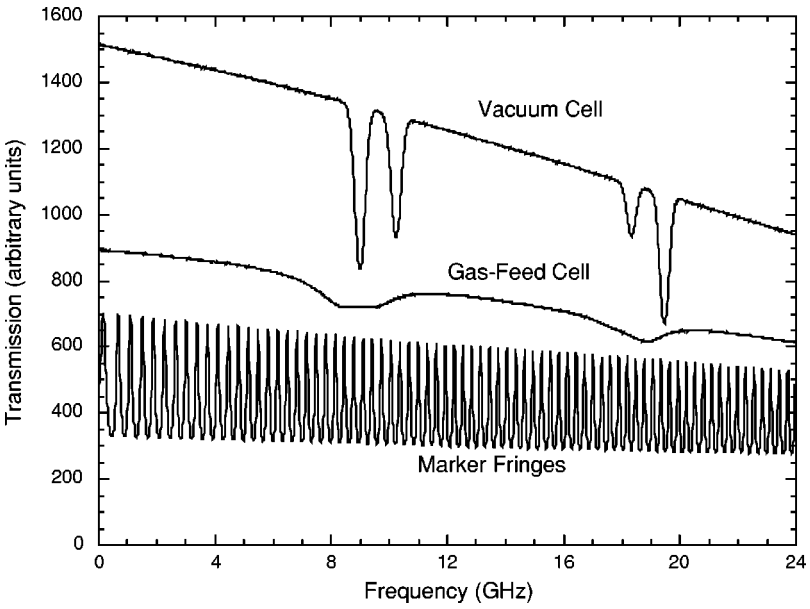

FIG. 1. Scan across the $D1$ hyperfine spectrum showing transmission through vapor cells at 21 °C with vacuum (top) and 80 Torr N_2 buffer gas (middle), along with marker fringes from the Fabry-Perot etalon (bottom). The intensity variation is due to a combination of varying laser current and etaloning effects. The frequency axis shown here is uncorrected, since the marker fringes are actually at equally spaced 300 MHz intervals.

strictly limited to somewhat less than 1 Torr (see Sec. V), with no possibility of major calibration errors as with more sophisticated devices.

In addition to the gas feed cell, a cesium vacuum cell (no buffer gas) was used to provide the zero-pressure reference for determining the pressure shift. This reference cell was arranged so that both the $D1$ and $D2$ lasers could pass through it onto separate photodiode detectors. The 894 nm $D1$ laser system was built in-house, using diffraction grating feedback in a Littrow configuration and an external cavity design with high passive stability [11]. It produced a single-mode output power of 20 mW, with a linewidth of less than 3 MHz and a continuous tuning range of over 25 GHz. The 852 nm $D2$ diode laser system was a commercial New Focus Model 6226 laser head in conjunction with a Model 6200 controller, which provided similar output characteristics.

For any line-shape measurement on strongly allowed transitions such as the $D1$ and $D2$, it is essential to reduce the intensity of the laser beams sufficiently to avoid any optical pumping effects, which show up as distinctive artifacts in the residuals of the fit. Thus, the beams were expanded to about 1 cm diameter and strongly attenuated using crossed calcite Glan-Thompson polarizers, supplemented by neutral-density attenuators. Measured intensities used in this experiment were about 100 nW/cm^2. A Melles Griot SuperBand optical spectrum analyzer, consisting of a scanning confocal Fabry-Perot etalon with a free-spectral range of 300 MHz, provided confirmation that each diode laser was operating in a single longitudinal mode. With its piezo scan halted, the etalon was used to provide marker fringes as the laser frequency was scanned during each line-shape measurement. This allowed determination and correction of any nonlinearity in the frequency scan as detailed in Sec. IV. The fringes were broadened by degrading the finesse of the etalon, using one mirror outside its intended wavelength range to give a finesse of roughly 20. This serves to eliminate aliasing effects caused by undersampling due to the limited number of data points in each scan.

III. DATA ACQUISITION

The data acquisition system consisted of a computer and 12-bit data acquisition board. A pair of digital-to-analog converter (DAC) outputs was used to scan the $D1$ or $D2$ laser across the transition, with typical scan widths of about 25 GHz for either laser, and 2000 data points taken in each scan. Data was simultaneously acquired for the gas-feed cell transmission, vacuum reference cell transmission, intensity normalization, and etalon marker fringes (see Fig. 1).

Each set of data for a particular gas and transition began with the apparatus pumped out to high vacuum with the gas line and cesium cell both closed off. Then the gas flow was started and the gas line, regulator, and oxygen/moisture trap were purged several times by filling with gas and then pumping it out through the vacuum system. After high vacuum was restored, the pumping line was closed off and the cesium cell was opened to the system. Then gas was admitted in roughly 10 Torr increments. At each pressure value, the gas feed was closed off to allow the system to reach equilibrium before a data scan was taken. The laser beam was blocked briefly using a mechanical shutter before each scan, to record any offsets in the detector readings.

The dominant instrumental effect present in the scans is the intensity variation of the laser beam on the detector as a function of frequency. For the 894 nm laser, some of this is due to the varying laser current as the frequency is scanned [11], but the New Focus 852 nm laser does not need to vary its current. A significant portion of the intensity variation comes from etalon effects caused by various elements in the optical path, such as attenuators, beam splitters, and windows. Typically, this results in a somewhat sinusoidal variation in intensity with frequency, with a period of several times the scan range (on the order of 100 GHz). There are often several competing elements which combine to make the total variation somewhat irregular.

Despite much effort to reduce these effects, in the end perhaps 5–10 % intensity variation over the scan would re-

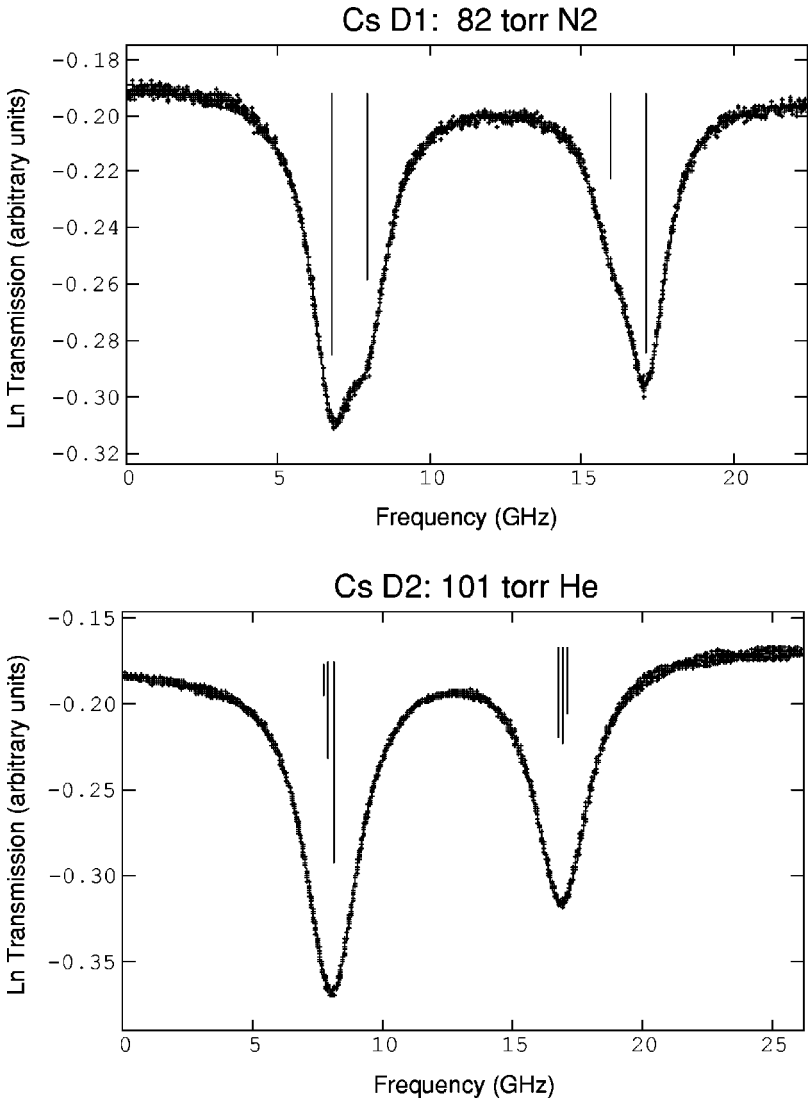

FIG. 2. Typical examples of the pressure broadening data for both $D1$ and $D2$ line in N_2 and He, shown within the fitting program following the complete iteration and parameter optimization cycle. The fitted curve itself is hidden by the data. The centers and relative magnitudes of the hyperfine components are shown by the lines within each peak.

main, almost always with slightly different shapes on the cell detector and the normalization detector. This made the normalization ineffective at removing the background, but another solution was found to work well. This was to move the vapor cell out of the beam path (by rotating the final L-shaped section of glass tubing about the O-ring joint) and then take a separate scan of the background alone. The backgrounds in scans with and without the cell typically match reasonably well, demonstrating that the cell itself is not causing significant etalon effects. The data can then be divided by this background (instead of by the normalization signal) during data analysis, thus removing the intensity variation quite effectively. The limiting factor in this process is that the laser frequency drifts slowly between consecutive scans, causing a slight mismatch during the background removal, so to minimize this effect background scans were taken once every five line-shape data scans.

IV. FITTING PROCEDURE

In order to extract the values of the pressure broadening and shift, a Voigt profile, which includes the appropriate hyperfine components, is fit to each absorption spectrum. A custom-written line-shape-fitting program performs a general nonlinear least-squares fit of a Voigt profile (Fig. 2). Fixed parameters in the fitting function include the ground- and excited-state hyperfine splittings, along with the relative strengths of each hyperfine component. Free parameters consist of the Lorentzian width (full width at half maximum), total scan range, frequency offset, and absorption coefficient, along with four parameters to define a third-order polynomial background on which the absorption peaks lie, to account for uncanceled background variation. Note that the frequency offset as defined here is the distance from the start of a scan to the center of the hyperfine spectrum.

For all fits presented here, the Doppler width was held as a fixed parameter and set to the calculated value for 21 °C. This is appropriate since the temperature variation during all of the data sets was less than ± 1 °C, so the Doppler width varies by less than $\pm 0.17\%$. Holding the Doppler width fixed greatly improves the quality of the fit to the Lorentzian, since there is substantial trade-off between the Doppler and Lorentzian widths. As for the absorption coefficient, it should equal $nL\sigma_0$, where n is the number density, L is the

TABLE I. Results and error analysis for the broadening (Lorentzian full width at half maximum) and shift of the Cs $D1$ and $D2$ spectral lines by N_2 and He buffer gases at pressures of 0–160 Torr. See the text for an explanation of the listed error values.

Buffer gas	Measured quantity	Value (MHz/Torr)	Linear fit error (MHz/Torr)	Voigt fit error (%)	Pressure error (%)	Total error (MHz/Torr and %)
N_2	$D1$ width	19.51	0.06	1.0%	0.6%	0.24=1.2%
N_2	$D1$ Shift	−8.23	0.02	0.14%	0.6%	0.05=0.6%
N_2	$D2$ Width	22.68	0.06	0.6%	0.6%	0.20=0.9%
N_2	$D2$ Shift	−6.73	0.01	0.10%	0.6%	0.04=0.6%
He	$D1$ Width	26.21	0.15	0.8%	0.6%	0.31=1.2%
He	$D1$ Shift	4.46	0.01	0.14%	0.6%	0.03=0.7%
He	$D2$ Width	23.50	0.06	0.6%	0.6%	0.21=0.9%
He	$D2$ Shift	0.75	0.004	0.12%	0.6%	0.006=0.8%

path length, and $\sigma_0=\int\sigma(\nu)d\nu=\pi cr_e f$ is the integral of the absorption cross section with r_e the classical electron radius and f the oscillator strength of the relevant transition. Thus, the absorption coefficient should remain constant for a set of scans at a fixed temperature but with different gas pressures, which provides a good cross-check as to the quality of the fits as the linewidths broaden.

The frequency axis was linearized using the marker fringes from the Fabry-Perot etalon. For broad fringes at low finesse, it is sufficient to do a five-point quadratic fit on each peak to extract the position of its center. Once this is done, a cubic fit to the fringe positions gives the nonlinearity of the frequency scale since the fringes are spaced at equal intervals. The absolute calibration of the linearized frequencies

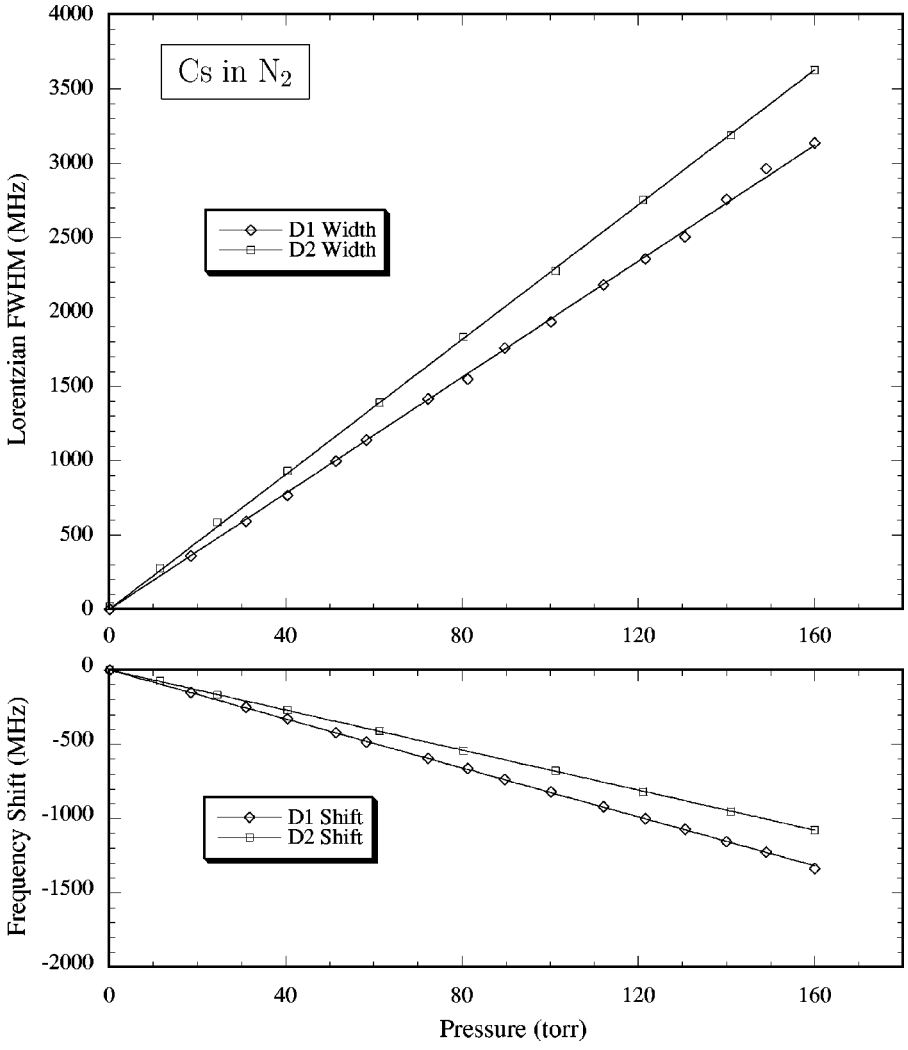

FIG. 3. Results for the pressure broadening and shift of the Cs $D1$ and $D2$ spectral lines in N_2 buffer gas at pressures of 0–160 Torr. Error bars on each point are smaller than the markers. Values are given in Table I.

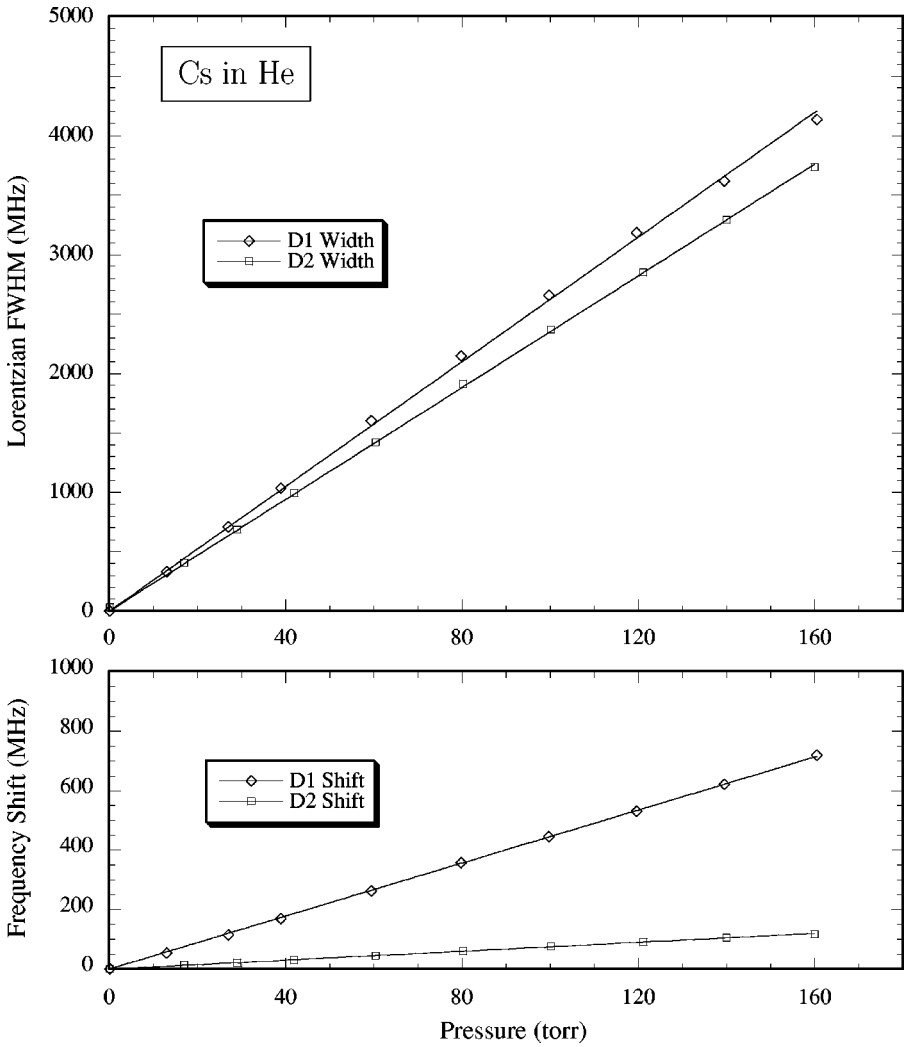

FIG. 4. Results for the pressure broadening and shift of the Cs $D1$ and $D2$ spectral lines in He buffer gas at pressures of 0–160 Torr. Error bars on each point are smaller than the markers. Values are given in Table I.

was determined in the fit to the vacuum cell spectra, using the total scan range as a free parameter, rather than by using the etalon free spectral range, since the value of 300 MHz is only approximate and was not separately measured to sufficient accuracy. The total scan range was determined for each vacuum cell spectrum and then subsequently held fixed in the corresponding fit for the buffer-gas cell, since the two frequency scales are common and the uncertainty in the scan range is lower for the vacuum cell fit.

In order to determine the shape of the background on which the absorption peaks are superimposed, a scan width of 25 GHz is adequate for buffer-gas pressures up to about 160–200 Torr. At higher pressures, this scan range becomes insufficient to recover fitted parameters with reasonable uncertainty. All fits used to determine the final shift and broadening results were taken at 160 Torr and below. The uncertainty in fitted line-shape parameters may also be improved by fixing the value of the absorption coefficient, since this remains constant; this was only done for $D1$ spectra recorded at high pressures ($>$120 Torr), using a value obtained from fits to $D1$ spectra at lower pressure.

V. RESULTS

Our results for the pressure broadening and shift of the Cs $D1$ and $D2$ spectral lines by N_2 and He buffer gases at pressures of 0–160 Torr are shown in Table I. The total uncertainty on each of the measured values is about 1%, with the uncertainties on the shifts generally smaller than those on the widths. The values for the pressure broadening are calculated by making one-parameter straight-line fits (constrained to pass through zero) to the measured Lorentzian widths as a function of pressure. The values for the pressure shift are similarly calculated using the difference between the frequency offsets of the gas-feed and reference cells in each scan. The straight-line fits to the data for N_2 are shown in Fig. 3 and for He in Fig. 4. Note that $D1$ data points above 140 Torr for N_2 and 120 Torr for He were obtained from fits in which the absorption coefficient was fixed, as described in Sec. IV, yet a consistent line is obtained if these points are omitted.

Two small but well-quantified corrections have been made to the fitted data sets. First is the correction of the manometer pressure readings, due to the thermal expansion of the mercury. The specific volume of mercury increases from 73.5560 ml/kg at 0 °C to 73.8367 ml/kg at 21 °C [12], an increase of 0.38%. Since 1 Torr is equal to 1 mm Hg at 0 °C, the true pressure (in Torr) is 0.38% lower than the manometer reading (in mm Hg) at 21 °C. The second correction involves the natural linewidth of 5 MHz and the laser line-

TABLE II. Comparison of pressure broadening and shift results presented here with previously published values. Broadenings and shifts are given in the standard units of $10^{-21}\,\mathrm{cm}^{-1}/\mathrm{cm}^{-3}$, equivalent to about 0.984 MHz/Torr at 21 °C.

Buffer gas	Pressure (Torr)	$D1$ (894.6 nm) Full width, γ/n ($10^{-21}\,\mathrm{cm}^{-1}/\mathrm{cm}^{-3}$)	$D1$ (894.6 nm) Shift, σ/n ($10^{-21}\,\mathrm{cm}^{-1}/\mathrm{cm}^{-3}$)	$D2$ (852.3 nm) Full width, γ/n ($10^{-21}\,\mathrm{cm}^{-1}/\mathrm{cm}^{-3}$)	$D2$ (852.3 nm) Shift, σ/n ($10^{-21}\,\mathrm{cm}^{-1}/\mathrm{cm}^{-3}$)	Reference	Instrumental resolution (MHz)
N_2	0–160	19.83 ± 0.24	-8.36 ± 0.05	23.05 ± 0.20	-6.84 ± 0.04	Present work	3
N_2	0–150	30.93 ± 5.71	-7.38 ± 0.11	39.38 ± 9.73	-7.25 ± 0.24	Ref. [4]	1500
He	0–160	26.64 ± 0.31	4.53 ± 0.03	23.88 ± 0.21	0.76 ± 0.01	Present work	3
He	0–150			25.05 ± 0.26	0.69 ± 0.03	Ref. [8]	40
He	0–24	24 ± 1	4.0 ± 0.2			Ref. [6]	140
He	200, 700	20.8 ± 3.2		24.2 ± 3.6		Ref. [5]	1500
He	0–150	19.49 ± 1.37	6.72 ± 1.02	27.20 ± 1.72	3.94 ± 1.71	Ref. [4]	1500
He	0–300 atm	29 ± 1	4.8 ± 0.2	26 ± 1	0.6 ± 0.2	Ref. [14]	6000

width of about 3 MHz which were simply subtracted from all of the Lorentzian widths prior to this fitting. Although quite small, this correction is necessary since the straight-line fits were constrained to pass through zero. An additional correction for the Cs-Cs resonance broadening is not necessary, since the broadening coefficient is roughly $6\times10^{-7}\,\mathrm{cm}^3\,\mathrm{s}^{-1}$ for both the $D1$ and $D2$ lines [13], thus contributing a width of only about 3 kHz at room temperature.

The various systematic and statistical uncertainties on our measured values are also given in Table I. The linear fit error is the calculated error on the straight line fits in Figs. 3 and 4. The Voigt fit error listed here is twice the maximum error on the fit for any single data point in each set, as given by the nonlinear least-squares fitting program (in percent). The calculation of this fitting error assumes purely statistical behavior of the data (i.e., that measurement errors are independent from point-to-point and normally distributed), which does not strictly hold for these data sets. Thus, we have chosen to double this calculated value to account for nonstatistical behavior and provide a conservative estimate of the errors. The pressure error simply assumes a worst-case error of up to 1 Torr on any pressure value, which would affect the slope of the fits by at most 0.6% over the range 0–160 Torr. The total error is the sum in quadrature of all these contributions, finally given as a percentage of the measured value in the last column of Table I.

Our results for the broadening and shift of the Cs $D1$ and $D2$ resonance lines by N_2 and He are compared with previously published values in Table II. Generally, our measurements show substantially improved precision, almost entirely due to the improvement in instrumental resolution. The recent work by Inoue *et al.* [8], also made using laser spectroscopy, achieves a similar level of precision; we note that the uncertainties quoted in this study do not include a large uncertainty in pressure readings, which the authors state could be as large as 10%. Our measurements are also generally in good agreement with previously published values, with the exception of those of Ref. [4]. Our numbers are even in good agreement with the early work of Garrett and Ch'en [14], which used a very low-resolution spectrometer and was primarily a high-pressure measurement, extrapolated to low pressures. Based on the good agreement with other authors, and on the significant improvement in experimental precision in our paper, it seems most reasonable to conclude that the large systematic uncertainty associated with deconvolution of the broad instrumental function was not completely accounted for in the values of Ref. [4]. This conclusion is supported by the good agreement with the high-precision values of Ref. [8] for $D2$ in He, given that our data acquisition and analysis procedure was the same for both He and N_2.

Considering the lack of other recent experimental measurements of the pressure broadening and shifts of cesium spectral lines, it may well be fruitful to pursue a more detailed and thorough investigation in the future. The requisite narrow-linewidth laser systems for the $D1$ and $D2$ will continue to be readily available. Most importantly, using the gas-feed system, it should be relatively simple to measure the pressure broadening and shift on both the $D1$ and $D2$ lines for a wide range of other gases, which are useful in optical pumping experiments, including H_2, Ne, Ar, Kr, and Xe. Other gases which have possible utility for optical pumping, such as CO, CO_2, CF_4, and SF_6, could also be used, although some of them might react unfavorably with the cesium vapor. Previous measurements for H_2 are limited to Ref. [4], while the noble gases have been done by that group along with Refs. [14–19] (also CF_4), Ref. [5] (only He, Ne, Ar, Kr), Refs. [6,7] (only He, Ne, Ar), and Ref. [8]. All of these measurements have experimental uncertainties in excess of 1%, and in most cases many times that.

VI. CONCLUSION

We have measured the pressure broadening and shift of the cesium $D1$ and $D2$ lines by N_2 and He buffer gases over the pressure range 0–160 Torr at 21 °C, using high-resolution laser spectroscopy with a pair of narrow-linewidth diode laser systems in order to eliminate the effects of the instrumental function on the line shapes. Although only a brief and preliminary study, our measurement has an uncertainty of about 1% for the broadenings, and somewhat better than 1%

for the shifts. In all cases, our values improve substantially upon those previously published, reducing the uncertainties by large factors and in some cases by more than one order of magnitude. Most importantly, previous values in the literature for the cesium $D1$ and $D2$ broadenings in N_2 have been reduced by 30–40 %, a correction which has been crucial for the proper computational modeling of our spontaneous polarization experiment [10].

ACKNOWLEDGMENTS

This measurement was done in the laboratory of Professor Norval Fortson at the University of Washington. We thank Blayne Heckel for the timely loan of the turbopump system, and Michael Romalis for numerous useful discussions. This project is supported by the National Science Foundation under Grant No. PHY-9732513.

[1] H. Margenau and W. W. Watson, Rev. Mod. Phys. **8**, 22 (1936).
[2] S. Y. Ch'en and M. Takeo, Rev. Mod. Phys. **29**, 20 (1957).
[3] N. Allard and J. Kielkopf, Rev. Mod. Phys. **54**, 1103 (1982).
[4] E. Bernabeu and J. M. Alvarez, Phys. Rev. A **22**, 2690 (1980).
[5] F. Siegling and K. Niemax, Z. Naturforsch. Teil A **39A**, 447 (1984).
[6] S. L. Izotova, N. I. Kaliteevskii, G. F. Lekhto, and M. S. Frish, Opt. Spektrosk. **59**, 484 (1985) [Opt. Spectrosc. **59**, 293 (1985)].
[7] S. L. Izotova, G. F. Lekhto, and M. S. Frish, Opt. Spektrosk. **59**, 228 (1985) [Opt. Spectrosc. **59**, 136 (1985)].
[8] Y. Inoue, K. Uchida, H. Hori, and T. Sakurai, J. Phys. Soc. Jpn. **59**, 516 (1990).
[9] W. M. Klipstein, S. K. Lamoreaux, and E. N. Fortson, Phys. Rev. Lett. **76**, 2266 (1996).
[10] A. Andalkar, R. B. Warrington, M. V. Romalis, S. K. Lamoreaux, B. R. Heckel, and E. N. Fortson, Phys. Rev. A **65**, 023407 (2002).
[11] A. Andalkar, S. K. Lamoreaux, and R. B. Warrington, Rev. Sci. Instrum. **71**, 4029 (2000).
[12] *CRC Handbook of Chemistry and Physics*, 81st ed., edited by D. R. Lide (CRC Press, Boca Raton, FL, 2000).
[13] Z. J. Jabbour, J. Sagle, R. M. Namiotka, and J. Huennekens, J. Quant. Spectrosc. Radiat. Transf. **54**, 767 (1995).
[14] R. O. Garrett and S. Y. Ch'en, Phys. Rev. **144**, 66 (1966).
[15] S. Y. Ch'en and R. O. Garrett, Phys. Rev. **144**, 59 (1966).
[16] S. Y. Ch'en, E. C. Looi, and R. O. Garrett, Phys. Rev. **155**, 38 (1967).
[17] R. O. Garrett S. Y. Ch'en, and E. C. Looi, Phys. Rev. **156**, 48 (1967).
[18] S. Y. Ch'en D. E. Gilbert, and D. K. L. Tan, Phys. Rev. **184**, 51 (1969).
[19] D. E. Gilbert and S. Y. Ch'en, Phys. Rev. **188**, 40 (1969).